Bulletin of Engineering Geology and the Environment (2022) 81: 43
https://doi.org/10.1007/s10064-021-02522-w

ORIGINAL PAPER

Effect of high temperature on pore characteristics, yield stress, and deformation property of sandstone

Weiqiang Zhang[1,2] · Zuoquan Wang[1] · Yi Du[3] · Shaoteng Zhang[1] · Zhoujian Shi[1] · Fanjia Li[4]

Received: 25 March 2021 / Accepted: 2 December 2021 / Published online: 27 December 2021

Abstract

High temperature can change rock structure and mechanical properties, which may cause potential hazards in rock engineering. In this paper, mercury intrusion porosimetry (MIP), uniaxial compression tests, P-wave velocity, and acoustic emission (AE) tests were implemented to study sandstone samples subjected to high temperatures. Results including the pore characteristic change, yield strength, and deformation of the sandstones after the high-temperature treatment were analyzed. The internal cause of the changes was revealed from the evolution of the microstructure obtained by the scanning electron microscope (SEM) test. The research results show a consistent critical temperature threshold in the changing process of pore characteristics, yield strength, and deformation characteristics of the sandstones, which is around 400 °C. When the heating temperature exceeds the threshold, the porosity of sandstone increases rapidly, the uniformity coefficient of pores increases sharply, the yield strength decreases rapidly, and the maximum displacement in the compaction stage increases significantly. Also, the number of big pores and the volume of pores with a diameter between 7 and 3000 nm were seen increasing. The above changes are mainly caused by the emergence of new cracks and the accelerated development of premier and new cracks in the microstructure of the sandstones, and the high temperature mainly affects pores with a diameter between 7 and 3000 nm. Although the yield strength decreases when the temperature goes beyond 400 °C, the ratio of the yield strength to the ultimate compressive strength remains nearly unchanged.

Keywords Sandstone · High temperature · Pore characteristics · Yield strength · Deformation property

Introduction

High temperature can affect the macroscopic and microscopic properties of the rock and bring about significant engineering effects (Liu et al. 2019a; Li et al. 2020; Martínez-Ibáñez et al. 2021; Peng et al. 2016; Ranjith et al. 2012). Therefore, the research on the pore characteristics and mechanical properties of rock undergone various high temperatures has very important theoretical significance and application value for deep rock engineering, such as geological storage of nuclear waste (Gens et al. 2009), exploitation of deep ore (Hassanzadegan et al. 2014; Zhang et al. 2008), underground gasification of coal mining (Liu et al. 2019b), safety and stability assessment of buildings and slope after fire disaster (Mónika 2002; Park et al. 2016; Sarro et al. 2021; Wu et al. 2013), and development of deep geothermal resources (Wang et al. 2020; Zhang et al. 2018).

Up to now, the research concerning the effect of high temperature on the macro-properties of rock mainly focuses on the physical and mechanical parameters (Brotóns et al.

✉ Weiqiang Zhang
zhangweiqiang1204@163.com

1 Institute of Mine Water Hazards Prevention and Controlling Technology, School of Resources and Geosciences, China University of Mining and Technology, Xuzhou, Jiangsu Province 221116, People's Republic of China

2 State Key Laboratory for Geomechanics and Deep Underground Engineering, China University of Mining and Technology, Xuzhou, Jiangsu Province 221116, People's Republic of China

3 State Key Laboratory of Continental Dynamics & National and Local Joint Engineering Research Center for Carbon Capture Utilization and Sequestration, Department of Geology, Northwest University, Xi'an, Shanxi Province 710069, People's Republic of China

4 School of Information and Control Engineering, China University of Mining and Technology, Xuzhou, Jiangsu Province 221116, People's Republic of China

2013; Tang et al. 2019; Vagnon et al. 2019, 2021), such as uniaxial compressive strength, elastic modulus, strain, wave velocity, and density. And, the most used research method is the laboratory test. According to the study results, as the heating temperature increases, the uniaxial compressive strength, elastic modulus, P-wave velocity, and bulk density of the specimen decrease gradually while the peak strain increases. Although many scholars have done a lot of research on this field, very few studies have been reported concerning the yield strength and the deformation in the compaction stage, indicating a research gap there. In the studies of high temperature affecting the microscopic properties of rocks, efforts were mainly made on understanding the microstructure changes of specific rocks at different temperatures using SEM tests (He et al. 2016; Lan et al. 2020; Meng et al. 2021; Zhang et al. 2021). However, only a few studies have focused on the pore characteristics (Castagna et al. 2018; Yao et al. 2021), which were more concentrated on the change of porosity (Géraud 1994; Zhang et al. 2016). Thus, much work on the distribution characteristics and evolution process of different types of pores after the high temperature is still needed. In addition, since the property of pores also has a significant influence on the permeability of rock (Darot et al. 1992; Liu et al. 2020; Sola and Rashidi 2008), it can be an important factor affecting the hydrological conditions of underground engineering. Therefore, it is necessary to carry out research on the evolution law of the pore characteristics and mechanical properties of rock subjected to high temperatures.

In order to investigate how high temperature affects the macroscopic properties and microstructure of the sandstone, we heated several groups of sandstone samples to different high temperatures. The mercury intrusion porosimetry (MIP), uniaxial compression test, P-wave velocity, and acoustic emission (AE) tests were used to analyze the variation of porosity, pore distribution, yield strength, and deformation properties of the sandstone samples. The scanning electron microscope (SEM) test was carried out to reveal the mechanisms behind the property changes. The research results can enrich theoretical research on the thermal damage of rock and provide basic data for rock engineering involving high-temperature environments.

Materials and methods

Preparation of rock samples

Sandstone is one of the most abundant rocks on the earth's surface and is frequently encountered in underground engineering, making it a good option for research. The test samples taken from a quarry of Jurassic strata in Shandong Province of China were dark red in the natural state and belonged to fine sandstone due to the grain size being between 0.08 and 0.20 mm. The sandstone was of clastic structure and contained granule and interstitial materials. The texture was relatively uniform, and there was no visible bedding. The cementation type of the samples was porous cementation, which is one of the most common cementation types in sedimentary rocks and features of the point contact relationship between mineral particles. The main minerals were feldspar (21%), quartz (66%), zeolite (5%), and calcite (6%). The samples for the test of mechanical properties were cut into standard $\Phi 50 \times 100$-mm cylinders (diameter and height), and the errors of diameter and height were within 0.3 mm and 5 mm, respectively. The end faces of the samples were perpendicular to the axis, and the non-parallelism and maximum deviation were smaller than 0.05 mm and 0.25°. The test sample of pore characteristics and microstructure was a small block whose diameter was 5 mm, and thickness was 3 mm.

Experimental procedure and instruments

This paper mainly deals with MIP, uniaxial compression, P-wave velocity, SEM, and AE tests. The uniaxial compression, AE, and P-wave velocity tests were implemented on the same sample, while MIP and SEM tests were carried out on separate samples. All the samples were pretreated by heating in a CTM300A high-temperature furnace produced by Weike Technology Company of Xuzhou, and the heating process was divided into three stages. First, for each group of sandstone samples, the rock samples were first heated at a rate of 5 °C/min until they reached the target temperature. Secondly, the samples were kept at the target temperature for 2 h to ensure the sample inside reached the same temperature and also to provide sufficient time for thermal reaction. Finally, the samples were cooled down to room temperature in the heating furnace at a rate of 0.5 °C/min, which helped maintain a uniform cooling pace inside and outside the samples. Also, it could reduce the influence on the physical and mechanical properties of samples owing to cooling. The samples tested by the uniaxial compression, AE, and P-wave velocity were heated to 15 temperature levels, which are 25 °C, 75 °C, 100 °C, 150 °C, 200 °C, 250 °C, 300 °C, 350 °C, 400 °C, 450 °C, 500 °C, 530 °C, 550 °C, 570 °C, and 600 °C, respectively. For each temperature level, three samples were prepared. The uniaxial compression and AE test were carried out on a WES-D1000 electro-hydraulic servo universal testing machine (Fig. 1a) with a micro-II digital AE system (Fig. 1e). The loading rate of uniaxial compression was 800 N/s, which was controlled by stress. The AE signal was monitored synchronously during the compression process, and the threshold value was set to 40 db. The P-wave velocity of samples was obtained by a RS-ST01C sound wave tester (Fig. 1d). When testing the P-wave velocity, Vaseline was applied between the probe and the sample to

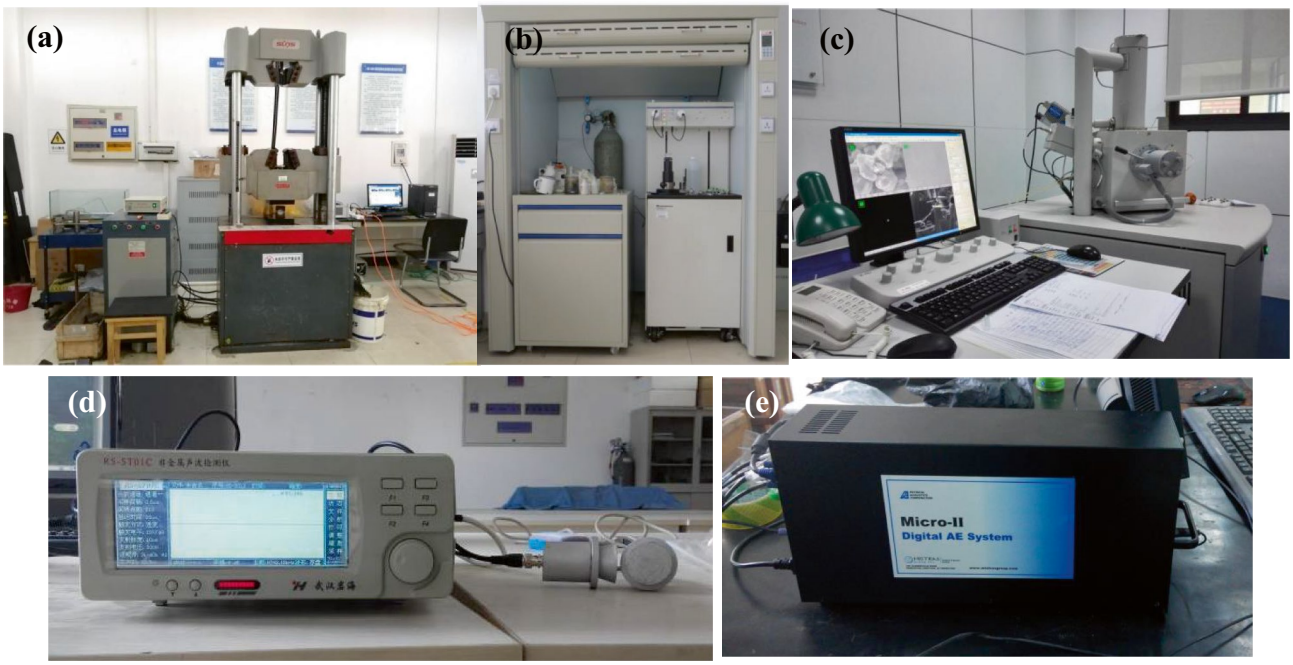

Fig. 1 Photos of main experimental instruments: **a** WES-D1000 electro-hydraulic servo universal testing machine; **b** AutoPore IV 9510 automatic mercury injection apparatus; **c** Quanta™ 250 SEM; **d** RS-ST01C sound wave tester; **e** micro-II digital AE system

increase the tightness of the contact. The ultrasonic wave was emitted by the transmitting probe and received by the receiving probe. The P-wave speed was calculated by the height of the samples and the time of the ultrasonic wave propagation in the samples. Considering the high cost of MIP and SEM tests, only six temperature levels were set in this test, which were 25 °C, 200 °C, 400 °C, 500 °C, 570 °C, and 600 °C, and one sample for each test. The MIP test was carried out on an AutoPore IV 9510 automatic mercury injection apparatus (Fig. 1b) produced by Micromeritics Instrument Company of America. The microscopic characteristics were observed using a Quanta™ 250 SEM (Fig. 1c).

Experimental results

Pore characteristics

The pore characteristics (i.e., pore diameter, volume, and porosity) of the sandstone samples were tested by MIP, in which the relationship between pore diameter and the applied pressure was in accordance with the Washburn equation (Zhang et al. 2017), as shown in Eq. (1).

$$P = -\frac{4\sigma \cos\theta}{r} \times 100\% \tag{1}$$

where P is the applied pressure; r is the diameter of pore in the sample; σ is the surface tension of mercury and equals 480 mN/cm; θ is the angle of the surface against the solid surface and equals to 140°.

The relationship between the pore volume and pore diameter of the samples is shown in Fig. 2. From the figure, the two properties have the same trend of change under the effect of high temperature. Specifically, both first increased at a low rate, then increased rapidly, and finally stabilized at a certain level. The pore diameters corresponding to the lower and upper limits of the rapid increase stage were 7 nm and 3000 nm, respectively. When the pore diameter was

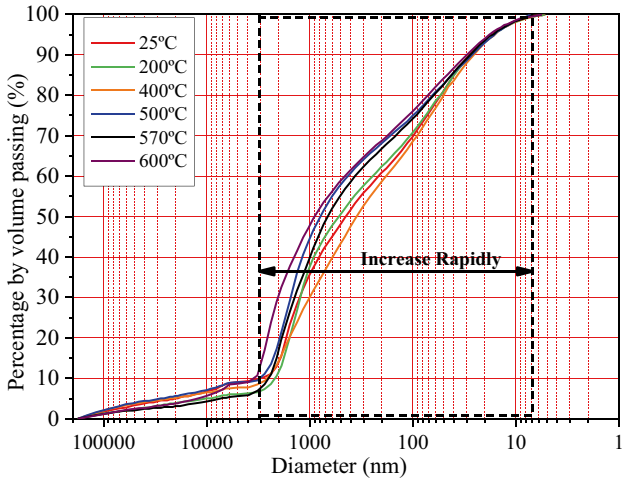

Fig. 2 Volume passing with pore diameter versus pore diameter

larger than 3000 nm, the pore volume increased slowly with the decrease of pore diameter. When the diameter was less than 7 nm, the pore volume remained almost unchanged. Besides, for pores between 7 and 3000 nm, the cumulative pore volume increased with the decrease of pore diameter, showing that the pores with diameters ranging from 7 to 3000 nm have significant distribution characteristics in the samples. As for samples subjected to temperatures below 400 °C, the cumulative pore volume of the samples had no obvious change in all pore diameters. Obviously, the effect of high temperature on the pore characteristics of sandstone is mainly reflected in the pores with a diameter of 7–3000 nm. This result can be verified by the study of Zhang et al. (2017), in which the peaks of incremental mercury intrusion distributed between 7 and 3000 nm were much higher than that at other pore diameters.

In order to study the distribution of pores with different sizes, the pores of sandstone samples were divided into five categories based on previous studies (Chen et al. 2013; Zhang et al. 2015a), which were large pores (diameter larger than 10,000 nm), big pores (diameter between 1000 and 10,000 nm), medium pores (diameter between 100 and 1000 nm), small pores (diameter between 10 and 100 nm), and micro-pores (diameter less than 10 nm). The pore volumes in each size range and under different temperatures are summarized (see Table 1 and Fig. 3). Apparently, the effects of high temperature varied with the pore size. The proportions of the large and micro-pores in the total pore volume were small, and their changes with the temperature were insignificant. The volume of big pores changed most significantly with the temperature, especially when the temperature went above 400 °C, and it was followed by medium pores. This is basically consistent with the research results of Zhang et al. (2017). In addition, the BMS (the total volume of big, medium, and small pores) was introduced to analyze the change of pore volume due to the effects of high temperature, as shown in Fig. 3. BMS occupied larger proportions in the total volume of pores, and it increased as the temperature increased. The rose of BMS above 400 °C was as high as 21.8%, which was far larger than 4.1% from 25 to 400 °C.

The relationship between the cumulative volume percentage of pores and diameter is shown in Fig. 2, which

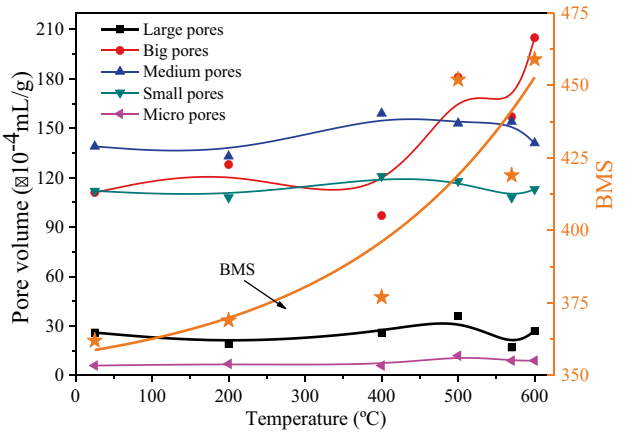

Fig. 3 Effect of temperature on the total volume of pores in different size categories, where BMS denotes the sum of the total volumes of big pores, medium pores, and small pores

shows that the distribution curves of samples heated by different temperatures are similar. In order to study the influence of temperature on the pores, uniformity coefficient (U_C) and curvature coefficient (C_C) were used to evaluate the variations of the pore diameter. Equations used to calculate the two coefficients are shown in Eqs. (2) and (3). U_C reflects the distribution range of pore diameters. The larger the value is, the more concentrated the pore diameters are. C_C reflects the smoothness of the curve. The specific data used for calculation is shown in Table 2. The calculation results are given in Fig. 4. In general, as the temperature increased, C_C kept stable (2.97 at 200 °C to 1.84 at 500 °C), while U_C changed significantly, especially at temperatures above 400 °C. When the temperature was below 400 °C, U_C fluctuated with the temperature increase, with a maximum of 0.11 at 200 °C and a minimum of 0.07 at 400 °C. When the temperature was higher than 400 °C, U_C increased drastically by 100%. Therefore, the pores become more and more unevenly distributed.

$$U_C = \frac{D_{60}}{D_{10}} \tag{2}$$

Table 1 The total volume of pores with different sizes and at different temperatures

Temperature /°C	Large pores ($\times 10^{-4}$ mL/g)	Big pores ($\times 10^{-4}$ mL/g)	Medium pores ($\times 10^{-4}$ mL/g)	Small pores ($\times 10^{-4}$ mL/g)	Micro-pores ($\times 10^{-4}$ mL/g)
25	26	111	139	112	6
200	19	128	133	108	7
400	26	97	159	121	6
500	36	181	153	118	12
570	17	157	154	108	9
600	27	205	141	113	9

Table 2 Summary of the results of percentage by volume passing

Temperature/°C	D_{10}/nm	D_{30}/nm	D_{60}/nm	U_C	C_C
25	2944	1262	214	0.07	2.53
200	2124	1223	237	0.11	2.97
400	2654	986	181	0.07	2.02
500	3115	1546	416	0.13	1.84
570	2511	1358	364	0.14	2.02
600	3230	1998	457	0.14	2.70

$$C_C = \frac{(D_{30})^2}{D_{10} \cdot D_{60}} \tag{3}$$

Porosity is an important parameter of rock pore and a significant parameter in hydrogeology for evaluating the water absorption capacity, water binding capacity, permeability, and so on. The variation of porosity of sandstone samples versus temperature is shown in Fig. 5 and Table 3. From Fig. 5, the changes of porosity can be divided into two phases: (1) when the temperature was lower than 400 °C, the porosity remained constant at a certain level, i.e., from 7.78% at 25 °C to 7.89% at 400 °C; (2) when the temperature exceeded 400 °C, the porosity increased rapidly with the temperature increase. When the temperature reached 600 °C, the porosity was 9.60%, which was 23.39% larger than it was at the room temperature.

P-wave velocity

According to the previous research results and relevant literature (Zhang et al. 2015b), the P-wave velocity can sensitively reflect the change of rock structure. Therefore, the changes of P-wave velocity of the samples were tested, and the results are given in Fig. 6, which shows that the wave

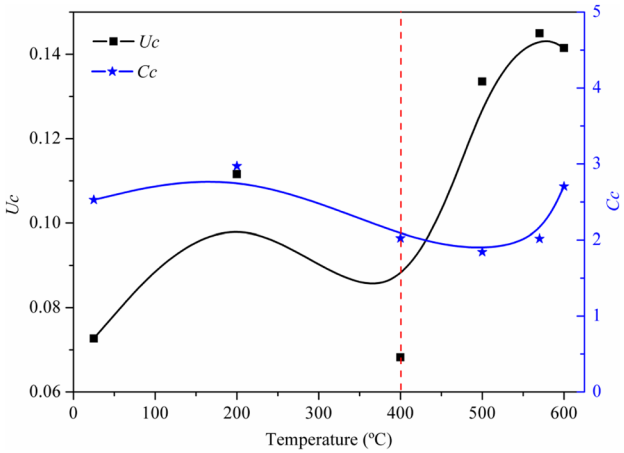

Fig. 4 Effect of temperature on the uniformity coefficient and curvature coefficient

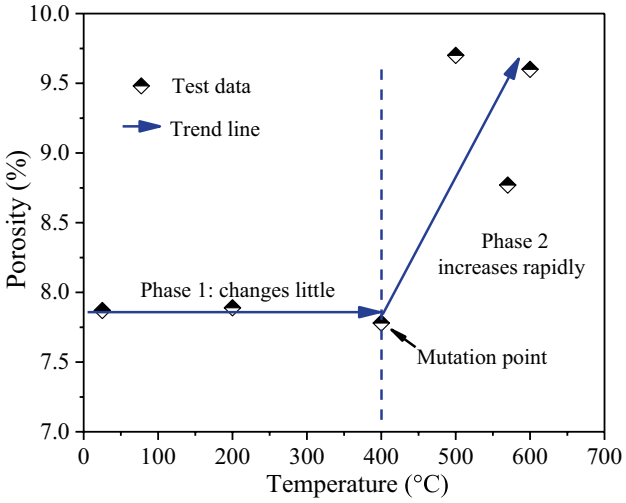

Fig. 5 Changes in porosity versus temperature

velocity gradually reduced with temperature increase, and the trend of the change can be divided into two phases. The P-wave velocity decreased slowly at a temperature below 400 °C, while at temperatures above 400 °C, the rate of decrease obviously accelerated, with the maximum rate reaching 43.4%. Comparing Figs. 5 and 6, it is found that the temperature corresponding to the changing point in P-wave velocity was the same as that of the porosity. Still, the changing trends of these two curves were opposite, indicating that the increase of porosity reduced the P-wave velocity. In order to analyze the internal relationship between porosity and P-wave velocity of the rock after high-temperature treatment, the P-wave velocity and the porosity at the same temperature are plotted, and the results are shown in Fig. 7. A good negative linear relationship between porosity and wave velocity exists, which can be expressed by Eq. (4)

$$N = 12.10 - 1.41 \times P \tag{4}$$

The correlation has a R^2 of 0.80, where N is porosity and P is P-wave velocity.

Stress and displacement

Figure 8 plots the stress and displacement curves of the sandstone samples. From the figure, all the curves share a similar growth trend except that of samples at 600 °C. The samples at temperatures other than 600 °C failed in the form of brittleness. The sample at 600 °C had a better ductility, whose maximum displacement was greater than those at other temperatures. On the other hand, it could be observed that there was an obvious compaction stage for each sample, which was significantly affected by the temperature. At 600 °C, the displacement was the largest, and the peak strength started to decrease quickly. The displacements of

Table 3 The porositys of sandstone samples undergone different temperatures

Temperature/°C	25	200	400	500	570	600
Porosity/%	7.87	7.89	7.78	9.70	8.77	9.60

the compaction stage of each sample under the influence of temperatures are shown in Table 4.

Figure 9 plots the changes in the average value of the maximum displacement (MD) of samples in the compression stage against the temperature. Notably, the MD increased with the increase of temperature. In detail, the MD of rock samples was higher at a temperature below 100 °C, but it reduced at the temperature from 100 to 200 °C, which was mainly caused by the natural variability of samples. ξ is a newly introduced value used to represent the change rate of displacement in the compaction stage, and it can be calculated using Eq. (5).

$$\xi_i = \frac{S_{i2} - S_{i1}}{\Delta T} \times 100\% \tag{5}$$

where S_{i1} is the displacement in the compaction stage at temperature T_{i1}, and S_{i2} is the displacement in compaction stage at temperature T_{i2} and $\Delta T = T_{i2} - T_{i1}$.

According to Eq. (5), ξ_1 (from 200 to 500 °C) and ξ_2 (from 530 to 600 °C) can be calculated as below:

$$\xi_1 = \frac{0.54 - 0.24}{300} \times 100\% = 0.10\% \tag{6}$$

$$\xi_2 = \frac{0.85 - 0.45}{70} \times 100\% = 0.57\% \tag{7}$$

From room temperature to 200 °C, ξ decreases with the temperature. When the temperature is in the range of 200 to 500 °C, ξ increases with the temperature at a steady but relatively low rate. When the temperature exceeds 530 °C, ξ increases with temperature at a much higher rate that is 5.7 times of the former.

Yield strength

The strength corresponding to the yield point of rock is called yield strength. When the stress exceeds the yield point, many cracks appear, and rock failure tends to occur. The occurrence of cracks can form AE signals, making AE information a good indication of the yield point (Kong et al. 2018; Sun et al. 2021). The specific method to identify the yield point of rock is to find the changing point of the AE count rate and the cumulative energy curve. Compared with the uniaxial compressive strength, yield strength can better reflect the compressive properties of sandstone in nature under the action of stress.

The variation of yield strength with temperature is shown in Fig. 10. From the figure, the yield strength curve can be divided into two phases according to the changing trend of yield strength: (1) from room temperature to 400 °C, the yield strength decreased slowly by 9.8%, from 66.2 MPa at 25 °C to 59.7 MPa at 400 °C; (2) from 400 to 600 °C, the yield strength decreased drastically by 29.3%, with a yield strength of 42.2 MPa at 600 °C. At a given temperature, taking R as the ratio of the yield strength to the peak strength, then we have

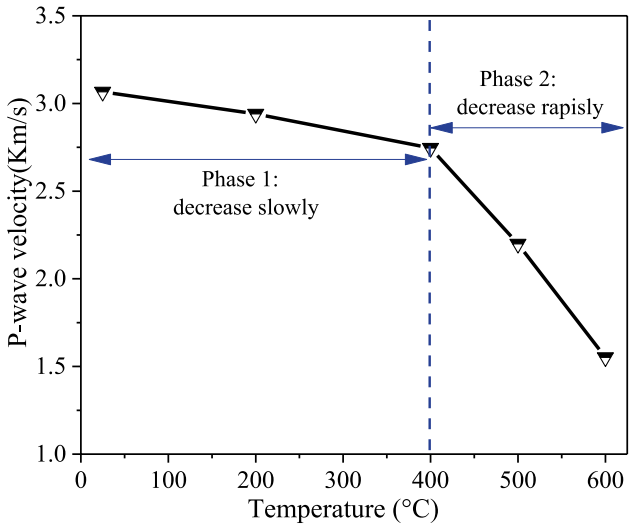

Fig. 6 Changes in the P-wave velocity versus temperature

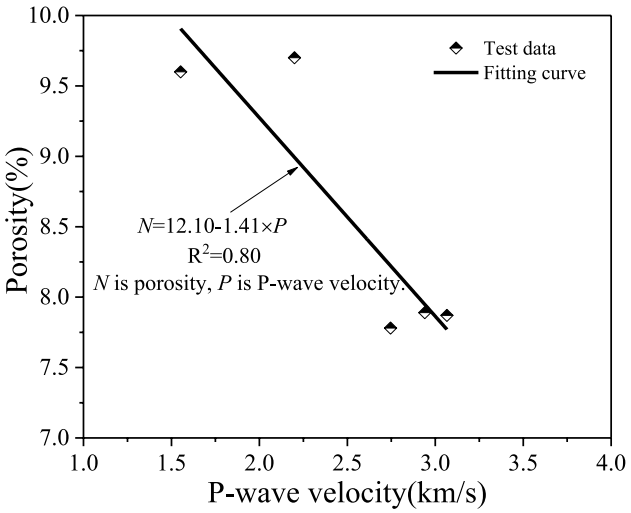

Fig. 7 The relationship between porosity and P-wave velocity

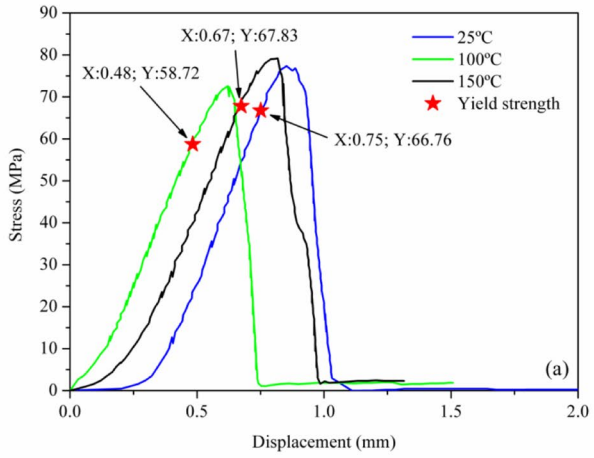

(a)

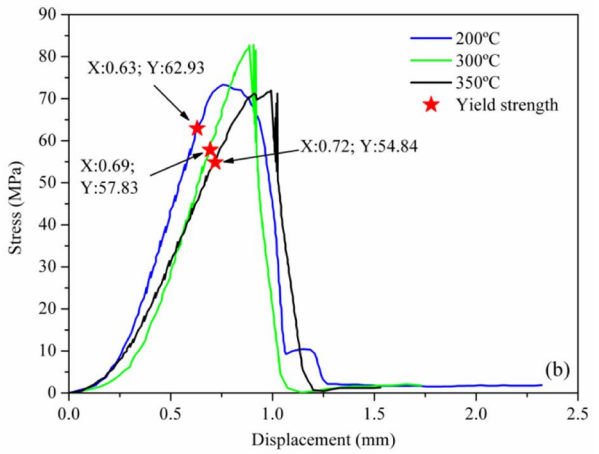

(b)

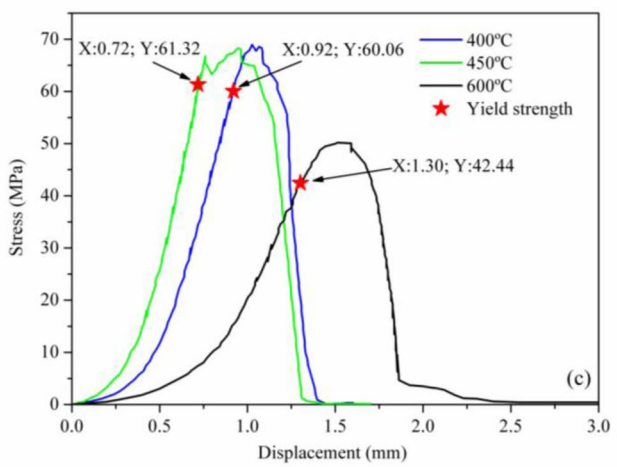

(c)

Fig. 8 The relationship between stress and displacement of part samples. **a** 25, 100, and 150 °C; **b** 200, 300, and 350 °C; **c** 400, 450, and 600 °C

Table 4 The displacements in the compaction stage of samples heated by different temperatures

Temperature /°C	Displacement of compression stage/mm				
	1	2	3	Average	Standard deviation
25	0.34	0.41	0.37	0.37	0.03
75	0.71	0.36	0.42	0.50	0.15
100	0.22	0.24	0.16	0.21	0.03
150	0.21	0.28	0.26	0.25	0.03
200	0.27	0.18	0.26	0.24	0.04
300	0.31	0.70	0.36	0.46	0.17
350	0.55	0.57	0.33	0.48	0.11
400	0.44	0.72	0.51	0.56	0.12
450	0.76	0.36	0.42	0.51	0.18
500	0.44	0.67	0.51	0.54	0.10
530	0.42	0.38	0.55	0.45	0.07
550	0.60	0.52	0.57	0.56	0.03
570	0.54	0.79	0.61	0.65	0.11
600	0.77	0.84	0.94	0.85	0.07

$$R = \frac{\sigma_Y}{\sigma_P} \tag{8}$$

where σ_Y is the yield strength at the given temperature and σ_P is the peak strength. As shown in Fig. 9, R ranged from 0.70 to 0.90 (as shown in Table 5). Obviously, the curve remains stable except at 300 °C. Therefore, although the temperature significantly impacted yield strength and peak strength, it had little influence on R.

The previous research has shown that the P-wave velocity is a parameter that can well reflect the damage of rock structure and the change of macro physical–mechanical

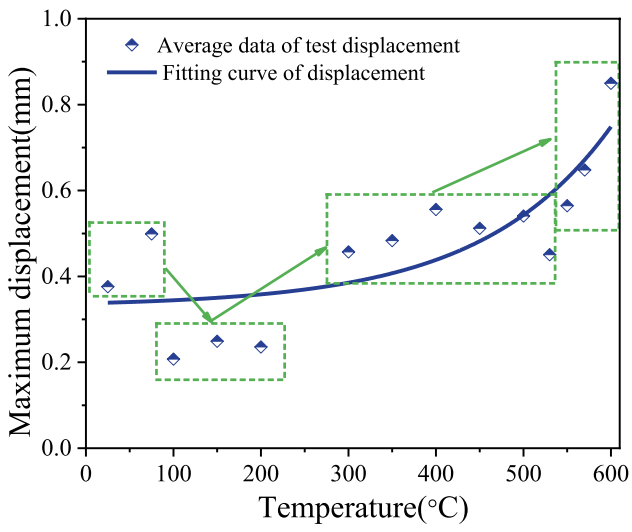

Fig. 9 The average value of maximum displacement in the compaction stage versus temperature

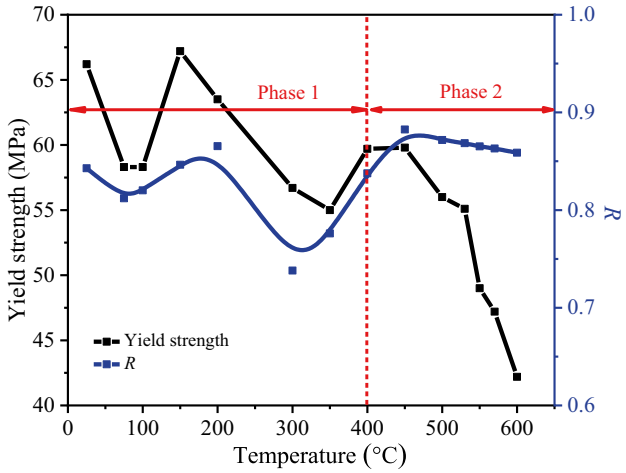

Fig. 10 The average yield strength versus temperature

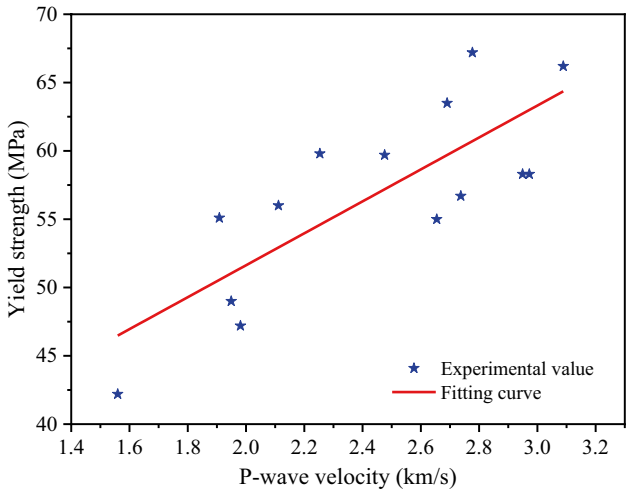

Fig. 11 The relationship between the average value of P-wave velocity and yield strength

parameters (Brotóns et al. 2013; Vagnon et al. 2019; Zhang et al. 2015b, 2017). Therefore, the relationship between the yield strength and P-wave velocity of this study was analyzed (see Fig. 11), which gave a moderate linear relation between them. The fitting equation is shown in Eq. (9), whose relation coefficient (R^2) is 0.63. The fitting line shows that the yield strength increases linearly as the P-wave velocity increases.

$$\sigma_Y = 11.69 \cdot v + 28.25 \tag{9}$$

where σ_Y is yield strength and v is wave velocity.

Microstructure

Structure change is the essence of rock damage, and SEM is an effective method to observe the microstructure of materials (He et al. 2016). Therefore, SEM tests were conducted on rock samples at different temperatures. The results are shown in Fig. 12. In the sandstone with a clastic structure, the mineral particles contacted with each other and the interstitial materials filled the pores and contact areas. The crystals looked relatively complete, but many of them had some micro defects, such as the circular or elliptical pores that could be observed at the surface. A small amount of premier cracks existed between the minerals (Fig. 12a and b). Micro-cracks with very small length and width were also found in some mineral crystals (Fig. 12a and c). In general, the microstructures of the sample did not change significantly below 400 °C. With the temperature increase, the premier cracks developed, and some new cracks emerged and extended, especially when the temperature was up to 400 °C. The surface layer of some minerals had fallen off (Fig. 12d), especially at the cross part of minerals, which might be caused by the stress concentration. When the temperature reached 570 °C, the majority of cracks in crystals started to connect with the existing cracks between the mineral particles (Fig. 12e). The number of transcrystalline cracks in the microstructure increased significantly at 600 °C (Fig. 12f), resulting in damages or even destructions to the crystal structure of some minerals. On the other hand, many connections were observed between the cracks, and the surface of some crystals was seen slightly rough.

Response characteristics of micro- and macro-properties

By comparing and analyzing the changes in the microstructure, pore characteristics, and mechanical properties of the sample, it can be seen that the premier cracks, including those in crystals, expanded in length and width, and new cracks emerged and extended which changed the distribution of pores. The increase of pore volume (7–3000 nm), uniformity

Table 5 The displacements in the compaction stage of samples heated by different temperatures

Temperature/°C	25	75	100	200	300	400	450	500	530	550	570	600
Yield strength/MPa	66.20	58.30	58.30	67.20	63.50	56.70	55.00	59.70	59.80	56.00	55.10	49.00
Peak strength/MPa	78.55	71.80	71.08	79.39	73.38	76.82	70.87	71.27	67.76	64.24	63.44	56.63
R	0.84	0.81	0.82	0.85	0.87	0.74	0.78	0.84	0.88	0.87	0.87	0.87

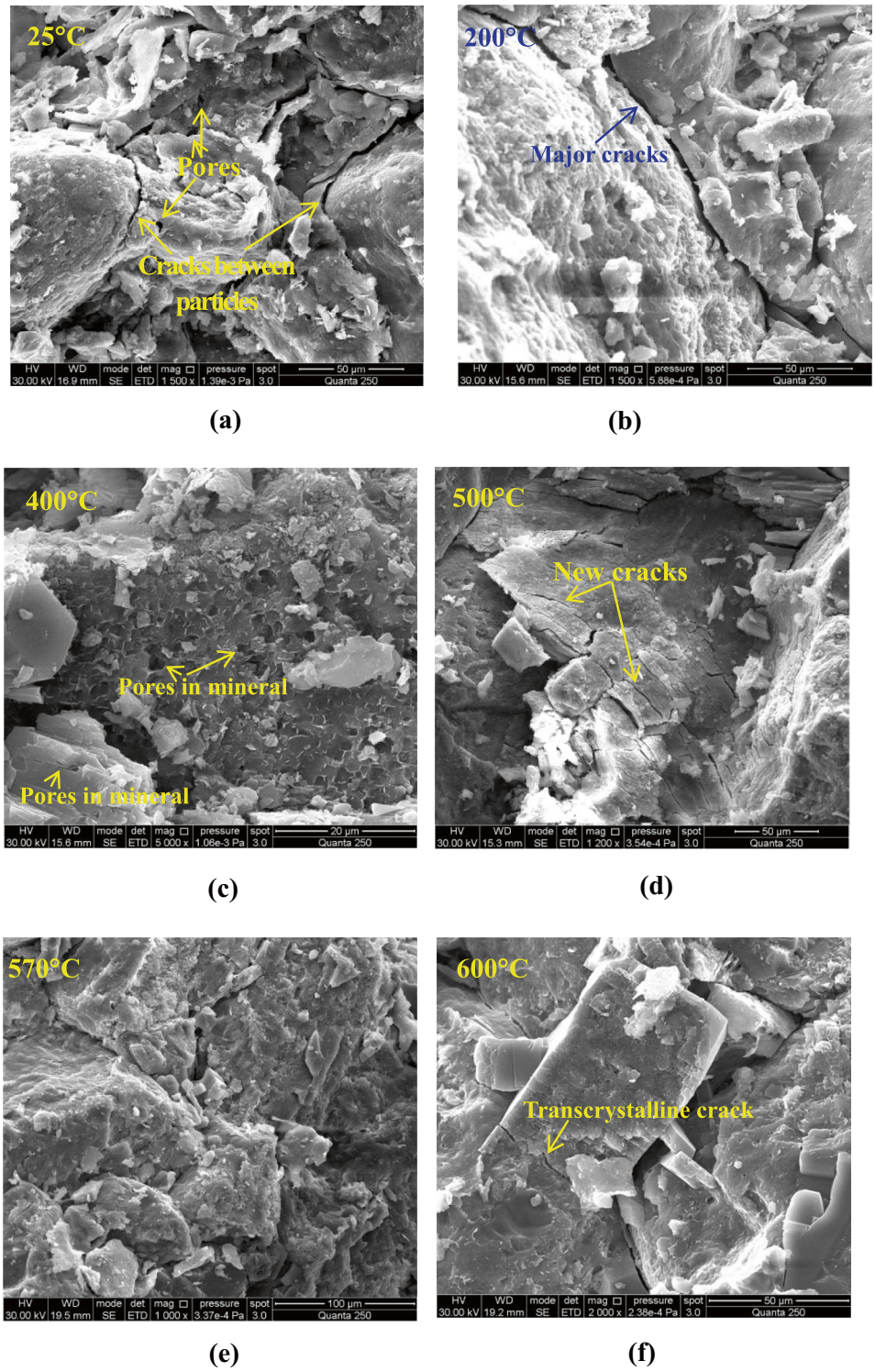

Fig. 12 The SEM images of samples. **a** 25 °C; **b** 200 °C; **c** 400 °C; **d** 500 °C; **e** 570 °C; **f** 600 °C

coefficient, and porosity was closely related to the generation of new cracks and the development of original cracks. The yield strength and maximum displacement of the compaction stage were also mainly determined by the shape, length, and connection of the cracks. From room temperature to 400 °C, the cracks developed slightly, and only a few new cracks were generated, leading to little change in the yield strength and maximum displacement of the compaction stage. While the rapid decrease of yield strength and the fast increase of the maximum displacement of the compaction stage was caused by the acceleration of crack development, the occurrence of new cracks, and the structure changing. The changes of

microstructure, pore characteristics, and mechanical properties of sandstone around 600 °C were more obvious, which was related to the phase transition of quartz around 573 °C (Sun and Zhang 2019). In the process of phase transformation, the volume of quartz expanded rapidly, causing compressive or tensile stresses on the surrounding mineral crystals. Cracks occurred when the stress exceeded the ultimate strength of the mineral crystals. The development of cracks reduced the yield strength of the sample and increased its plasticity, which was also the main reason for the increase of the maximum displacement in the compaction stage.

Conclusions

In order to evaluate the influence of high temperature on sandstone, the SEM test was adopted to analyze parameters, including the pore distribution, porosity, yield strength, and displacement in the compression stage of some sandstones at different temperatures. The main conclusions were as below:

(1) The critical temperature threshold at which the pore characteristics of sandstone change significantly is about 400 °C. After this point, the volume of the pores with a diameter of 7–3000 nm increases significantly, the porosity increases rapidly, the number of big pores increases significantly, and the uniformity coefficient increase quickly.
(2) In general, the maximum displacement in the compaction stage increases with temperature, especially at above 500 °C, which is caused by the occurrence of new cracks.
(3) The sandstone has a good yield strength in nature, and it decreases with the heating temperature, especially at temperatures above 400 °C. The temperature almost has no influence on the rate of yield strength and peak strength. The main reasons for the decrease of yield strength are the emergence of new cracks, the development of premier, and new cracks and the decomposition of cement.
(4) A moderate linear relationship exists between the wave velocity and yield strength.

Funding This study is funded by "the National Natural Science Foundation of China (Grant No. 41807233)", "the Natural Science Foundation of Jiangsu Province (Grant No. BK20180662)," the Priority Academic Program Development of Jiangsu Higher Education Institutions, and Postgraduate Research & Practice Innovation Program of Jiangsu Province (KYCX21_2247).

References

Brotóns V, Tomás R, Ivorra I, Alarcón JC (2013) Temperature influence on the physical and mechanical properties of a porous rock: San Julian's calcarenite. Eng Geol 167:117–127. https://doi.org/10.1016/j.enggeo.2013.10.012

Chen SB, Xia XH, Qin Y (2013) Classification of pore structures in shale gas reservoir at the Longmaxi formation in the south of Sichuan basin. J China Coal Soc 38:760–765

Castagna A, Ougier-Simonin A, Benson PM, Browning J, Walker RJ, Fazio M, Vinciguerra S (2018) Thermal damage and pore pressure effects of the brittle-ductile transition in Comiso limestone. J Geophys Res Solid Earth 123(9):7644–7660. https://doi.org/10.1029/2017JB015105

Darot M, Gueguen Y, Baratin ML (1992) Permeability of thermally cracked granite. Geophys Res Lett 19(9):869–872. https://doi.org/10.1029/92GL00579

Géraud Y (1994) Variations of connected porosity and inferred permeability in a thermally cracked granite. Geophys Res Lett 21(11): 979–982. https://www.researchgate.net/publication/241062848

Gens A, Garitte B, Olivella S, Vaunat J (2009) Applications of multiphysical geomechanics in underground nuclear waste storage. Eur J Environ Civ En 13:937–962. https://doi.org/10.1080/19648189.2009.9693162

Hassanzadegan A, Blöcher G, Milsch H, Urpi L (2014) The effects of temperature and pressure on the porosity evolution of Flechtinger sandstone. Rock Mech Rock Eng 47:421–434. https://doi.org/10.1007/s00603-013-0401-z

He ZG, Lin GS, Tian SC, Wang HZ, Shen ZH, Li JB (2016) SEM analysis on rock failure mechanism by supercritical CO2 jet impingement. J Petrol Sci Eng 146:111–120. https://doi.org/10.1016/j.petrol.2016.04.023

Kong B, Li ZH, Wang EY (2018) Fine characterization rock thermal damage by acoustic emission technique. J Geophys Eng 15(1):1–12. https://doi.org/10.1088/1742-2140/aa9a54

Liu P, Cui SG, Li ZH, Xu XF, Guo C (2019a) Influence of surrounding rock temperature on mechanical property and pore structure of concrete for shotcrete use in a hot-dry environment of high-temperature geothermal tunnel. Constr Build Mater 207:329–337. https://doi.org/10.1016/j.conbuildmat.2019.02.125

Liu XP, Guo GL, Li HZ (2019b) Study on the propagation law of temperature field in surrounding rock of underground coal gasification (UCG) combustion cavity based on dynamic thermal parameters. Results Phys 12:1956–1963. https://doi.org/10.1016/j.rinp.2019.02.006

Lan WJ, Wang HX, Zhang X, Fan HB, Feng K, Liu YX, Sun BY (2020) Investigation on the mechanism of micro-cracks generated by microwave heating in coal and rock. Energy 206:118211. https://doi.org/10.1016/j.energy.2020.118211

Li M, Wang DM, Shao ZL (2020) Experimental study on changes of pore structure and mechanical properties of sandstone after high-temperature treatment using nuclear magnetic resonance. Eng Geol 275:105739. https://doi.org/10.1016/j.enggeo.2020.105739

Liu JR, Shi WX, Wu XR (2020) Experimental study on thermally enhanced permeability of rock with chemical agents. J Petrol Sci Eng 195:107895. https://doi.org/10.1016/j.petrol.2020.107895

Mónika H (2002) Changes in sandstones of historical monuments exposed to fire or high temperature. Fire Tech 38:373–382. https://doi.org/10.1023/A:1020174500861

Martínez-Ibáñez V, Garrido ME, Hidalgo Signes C, Basco A, Miranda T, Tomás R (2021) Thermal effects on the drilling performance of a limestone: relationships with physical and mechanical properties. Appl Sci 11(7):3286. https://doi.org/10.3390/app11073286

Meng T, Xue YB, Ma JW, Yue Y, Liu W, Zhang J, Li EB (2021) Evolution of permeability and microscopic pore structure of sandstone and its weakening mechanism under coupled thermo-hydro-mechanical environment subjected to real-time high temperature. Eng Geol 280:105955. https://doi.org/10.1016/j.enggeo.2020.105955

Park JW, Rutqvist J, Ryu D, Park ES, Synn JH (2016) Coupled thermal-hydrological-mechanical behavior of rock mass surrounding a

high-temperature thermal energy storage cavern at shallow depth. Int J Rock Mech Min 83:149–161. https://doi.org/10.1016/j.ijrmms.2016.01.007

Peng J, Rong G, Cai M, Yao MD, Zhou CB (2016) Physical and mechanical behaviours of a thermal-damaged coarse marble under uniaxial compression. Eng Geol 200:88–93. https://doi.org/10.1016/j.enggeo.2015.12.011

Ranjith PG, Daniel RV, Chen BJ, Perera MSA (2012) Transformation plasticity and the effect of temperature on the mechanical behavior of Hawkesbury sandstone at atmospheric pressure. Eng Geol 151:120–127. https://doi.org/10.1016/j.enggeo.2012.09.007

Sola BS, Rashidi F (2008) Experimental study of hot water injection into low-permeability carbonate rocks. Energ Full 22:2353–2361. https://doi.org/10.1021/ef800009r

Sun Q, Zhang YL (2019) Combined effects of salt, cyclic wetting and drying cycles on the physical and mechanical properties of sandstone. Eng Geol 248:70–79. https://doi.org/10.1016/j.enggeo.2018.11.009

Sarro R, Pérez-Rey I, Tomás R, Alejano LR, Hernández-Gutiérrez LE, Mateos RM (2021) Effects of wildfire on rockfall occurrence: a review through actual cases in Spain. Appl Sci 11:2545. https://doi.org/10.3390/app11062545

Sun H, Ma LQ, Liu W, Spearing AJS, Han J, Fu Y (2021) The response mechanism of acoustic and thermal effect when stress causes rock damage. Appl Acoust 180:108093. https://doi.org/10.1016/j.apacoust.2021.108093

Tang ZC, Sun M, Peng J (2019) Influence of high temperature duration on physical, thermal and mechanical properties of a fine-grained marble. Appl Therm Eng 156:34–50. https://doi.org/10.1016/j.applthermaleng.2019.04.039

Vagnon F, Colombero C, Colombo F, Comina C, Ferrero AM, Mandrone G, Vinciguerra SC (2019) Effects of thermal treatment on physical and mechanical properties of Valdieri Marble - NW Italy. Int J Rock Mech Min 116:75–86. https://doi.org/10.1016/j.ijrmms.2019.03.006

Vagnon F, Colombero C, Comina C, Ferrero AM, Mandrone G, Roseane M, Vinciguerra SC (2021) Relating physical properties to temperature induced damage in carbonate rocks. Géotech Lett 11(1):1–11. https://doi.org/10.1680/jgele.20.00122

Wu G, Wang Y, Swift G, Chen J (2013) Laboratory investigation of effects of temperature on the mechanical properties of sandstone. Geotech Geol Eng 31:809–816. https://doi.org/10.1007/s10706-013-9614-x

Wang YJ, Jiang JY, Darkwa J, Xu ZY, Zheng XF (2020) Experimental study of thermal fracturing of Hot Dry Rock irradiated by moving laser beam: temperature, efficiency and porosity. Renew Energ 160:803–816. https://doi.org/10.1016/j.renene.2020.06.138

Yao JH, Tao M, Zhao R, Hashemi SS, Wang YQ (2021) Effect of microwave treatment on thermal properties and structural degradation of red sandstone in rock excavation. Miner Eng 162:106730. https://doi.org/10.1016/j.mineng.2020.106730

Zhang Y, Zhao YS, Wan ZJ (2008) Experimental study on effect pore pressure on feldspar fine sandstone permeability under different temperatures. Chin J Rock Mech Eng 27:53–58

Zhang YL, Sun Q, Li JX, Zhang WQ (2015a) Pore and Mechanical characteristics of high-temperature baked clay (in Chinese). Chinese J Rock Mech Eng 34:1480–1488

Zhang WQ, Qian HT, Sun Q, Chen YH (2015b) Experimental study of the effect of high temperature on primary wave velocity and microstructure of limestone. Environ Earth Sci 74:5739–5748

Zhang R, Ning Z, Yang F, Zhao H, Wang Q (2016) A laboratory study of the porosity-permeability relationships of shale and sandstone under effective stress. Int J Rock Mech Min 81:19–27. https://doi.org/10.1016/j.ijrmms.2015.11.006

Zhang YL, Sun Q, He H, Cao LW, Zhang WQ, Wang B (2017) Pore characteristics and mechanical properties of sandstone under the influence of temperature. Appl Therm Eng 117:537–543. https://doi.org/10.1016/j.applthermaleng.2016.11.061

Zhang SK, Huang ZW, Zhang HY, Guo ZQ, Wu XG, Wang TY, Zhang CC, Xiong C (2018) Experimental study of thermal-crack characteristics on hot dry rock impacted by liquid nitrogen jet. Geothermics 76:253–260. https://doi.org/10.1016/j.geothermics.2018.08.002

Zhang L, Li HB, Sun ZM, Cao Y, Wang H (2021) Microstructural evolution of pseudotachylyte-bearing rocks during increasing temperatures: evidence from rock-heating experiments 149. https://doi.org/10.1016/j.jsg.2021.104398